Effect of Forced Gas Cooling on GTA Weld Pools

Forced convective cooling refines the weld metal macrostructure by changing the weld-pool geometry

BY M. E. WELLS AND W. E. LUKENS

ABSTRACT. A method has been developed to apply forced convection heat transfer by gas jet impingement to weld metals deposited by the GTAW process at heat inputs in excess of 100 kJ/in. (4 kJ/mm). The method involves the use of multiple gas jets directed at the surface of the weld pool to increase convective heat transfer, *i.e.*, forced convective cooling.

Autogenous bead-on-plate welds were made in a titanium alloy with and without forced convective cooling. All welding variables were maintained constant; only the introduction of the cooling gas during welding was different. The weld pool geometry, temperature distributions, macrostructure and microstructure of the welds were evaluated.

The results of visual and macrostructural observations indicate that forced convective cooling forms a refined weld metal macrostructure through control of the weld pool geometry. In addition to grain refinement, forced convective cooling modifies the shape of the weld bead. The depth-to-width ratio of the weld bead increases and the width of the weld HAZ decreases. The results of temperature measurements indicate that forced convective cooling increases the weld metal cooling rate. By increasing the cooling rate, the time at transformation is suppressed and a finer weld metal microstructure is produced. Additionally, the weld pool surface temperature decreases and thermal gradients near the solid-liquid interface also decrease.

Introduction

Background

High heat input welding processes offer the potential of significant advances in welding efficiency by reducing the number of welding passes and between-pass mechanical cleaning. It is estimated that a fifty percent decrease in welding costs can be achieved by utilization of higher heat input values and deposition rates (Ref. 1). However, the solidification structure of the fusion zone is influenced by the magnitude and duration of the weld thermal cycle (Refs. 2, 3). High heat inputs into the fusion zone and corresponding slow cooling rates result in increased solidification times for grain growth. As the weld solidification structure coarsens and various segregation mechanisms have time to to develop, the strength, toughness, and ductility of the weld deposit decreases (Refs. 2, 3). As a result, limitations on heat input are included in the process specifications of weldable alloys used in ship construction (Ref. 4). By developing a method to control the solidification structure of high heat input welds, it should be possible to reduce the labor costs of welding and improve the mechanical properties and fracture resistance of the weld metal deposit.

Control of the weld solidification structure has been attempted often in both ferrous and nonferrous alloys. Methods employed to date have fallen into either one of the two general categories of inoculation or dendrite fragmentation. Inoculation normally involves the introduction of minute quantities of high melting point particles into the trailing edge of the weld pool to act as nucleation sites for grain growth. Dendrite fragmentation resulting from electromagnetic stirring, arc oscillation, torch vibration or combinations of these involves the mechanical detachment of dendrite tips or the melting off of secondary dendrite arms to serve as nucleation points for new grains to grow. A review of these methods (Refs. 5-8) has shown that solidification control of high heat input welds is much more difficult due to the high temperatures and thermal gradients found in the weld pools—values of 1900°F/in. (41°C/mm) and above are reported in the literature (Ref. 5). For inoculation, high inoculant levels are required to generate sufficient cooling at the solid-liquid interface to protect the particles from melting. Although extensive grain refinement has been obtained using TiC, TiB_2 and TiC/Fe-Ti mixtures in mild steel (Ref. 6), and yttrium in titanium (Ref. 7), the loss of fracture toughness due to grain boundary embrittlement has limited the usefulness of this approach for high heat input processes. For dendrite fragmentation, high thermal gradients reduce the extent of supercooling, limiting dendrite tip growth, and fragments which are removed and swept into the bulk of the weld pool would most probably be remelted (Ref. 8).

An alternative approach investigated in this study involves the use of multiple gas jets directed at the surface of the weld pool to increase convective heat transfer, *i.e.*, forced convective cooling. Relatively large heat transfer coefficients have been obtained by multiple gas jets impinging on a solid surface (Fig. 1), while providing

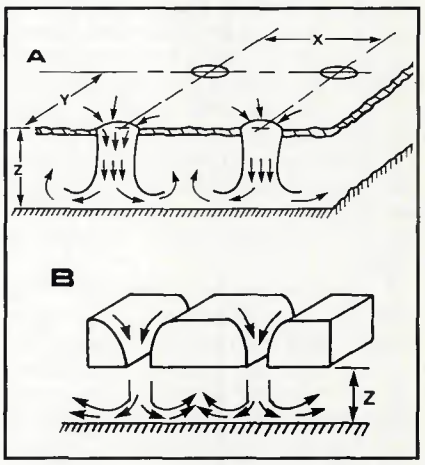

Fig. 1—Two alternative types of impinging jets commonly used in industry for cooling and heating of moving components. A—Array of round jets in thin plate; B—Array of parallel slot jets with bell-shaped inlets

M. E. WELLS and W. E. LUKENS are with the David Taylor Naval Ship Research and Development Center, Bethesda, Md.

a high degree of control of the surface heat transfer rate and distribution (Refs. 9–12). For the case of welding, increasing convective heat transfer is expected to extract heat quickly from the weld pool, providing temperature conditions more favorable for equiaxed grain growth. Additionally, enhanced cooling by jet impingement may reduce the time at transformation temperature and the time to cool to values more characteristic of lower heat input welds.

Although brief applications of forced convection heat transfer have been performed on aluminum weldments (Refs. 5, 13, 14), no studies have been performed on forced convective cooling of high heat input welds in any other alloy or on the metallurgical improvements that may result. The objective of this investigation is the application and evaluation of the effects of forced convection heat transfer on weld metals deposited by high heat input (>100 kJ/in., or 4 kJ/mm) welding processes. In this work, the temperature conditions in high heat input welds are examined, and the potential for weld modifications by forced convective cooling is discussed.

Weld Pool Solidification

Within and around the weld pool are a series of isotherms. One of these isotherms is the effective liquidus temperature of the alloy and corresponds to the weld pool/base metal interface. It is at this interface that solidification begins with the solid phase growing off of the partially melted base metal grains. This type of growth is referred to as epitaxial growth and is well documented in the welding literature (Refs. 3, 5, 15). The initial growth of partially melted grains in the base metal is usually followed by a period of columnar grain development which dominates the remainder of weld pool solidification. As the columnar grains grow into the fusion zone, their actual shape and size is determined by "competitive growth" (Ref. 3). This process depends on the geometry of the weld pool, as shown in Fig. 2. Grains growing in certain directions parallel to the maximum thermal gradient have a competitive advantage over less favorably oriented grains. This difference in columnar grain development for tear-shaped and elliptical weld pools has been demonstrated experimentally in several studies (Refs. 16, 17). The welding process determines how heat is introduced in the weld zone, and therefore the weld pool geometry.

The columnar structure may be cellular or dendritic, depending on the solidification conditions. Briefly, the mechanism of solidification is as follows. In most alloy systems, the solid is leaner in solute than the liquid in equilibrium with it, and as the weld metal cools through the solidification range, solute is rejected at the solid-liquid interface. Because the freezing process is so rapid that diffusional processes cannot effectively remove the excess solute, solute enrichment occurs at the solid-liquid interface until a dynamic equilibrium is reached (Ref. 16). The resulting dynamic equilibrium provides an excess of solute in the liquid near the interface, with the solute content decreasing to the nominal liquid composition at some distance from the interface—Fig. 3A. The concentration of the solute in the liquid at a distance x ahead of the interface is given by (Ref. 18)

$$C_\ell = C_o\left[1 + \frac{1-k_o}{k_o}\exp\left(-\frac{R}{D_1}x\right)\right] \quad (1)$$

where C_ℓ = concentration in liquid at a point x ahead of the interface
C_o = composition of the alloy
k_o = ratio of solute concentrations in solid and liquid
R = solidification rate
D_1 = diffusion coefficient in the liquid
x = distance ahead of interface

The effective liquidus temperature, T_e, is dependent on solute concentration in the liquid (Ref. 18). As the liquid is enriched due to rejection of solute at the solid-liquid interface, the effective liquidus temperature decreases ahead of the advancing interface. The effective liquidus temperature ahead of the interface is shown schematically in Fig. 3B and is given by

$$T_e = T_o - mC_\ell \quad (2)$$

where T_o = equilibrium melting point of the pure metal
m = slope of the liquidus line in the phase diagram

For any point x ahead of the interface, the effective liquidus temperature can be obtained by substituting Equation 1 into 2 and obtaining

$$T_e = T_o - mC_o\left[1 + \frac{1-k_o}{k_o}\exp\left(-\frac{R}{D_1}x\right)\right] \quad (3)$$

where T_e = effective liquidus temperature

The actual temperature, T, at any point in the liquid is given by

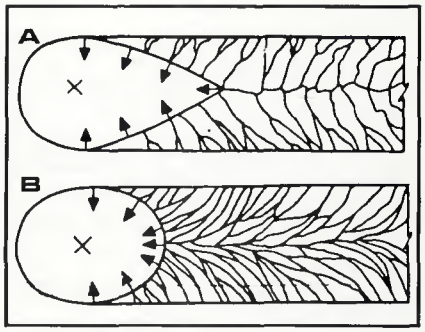

Fig. 2—Influence of weld pool geometry on solidification macrostructure. A—Columnar grain development in a tear-shaped weld pool. Arrows show the almost invariant direction of the maximum thermal gradient, resulting in early elimination of unfavorably oriented grains; B—Columnar grain development in an elliptical weld pool. Progressive change in direction of the maximum thermal gradient is reflected in the survival of many more columnar grains

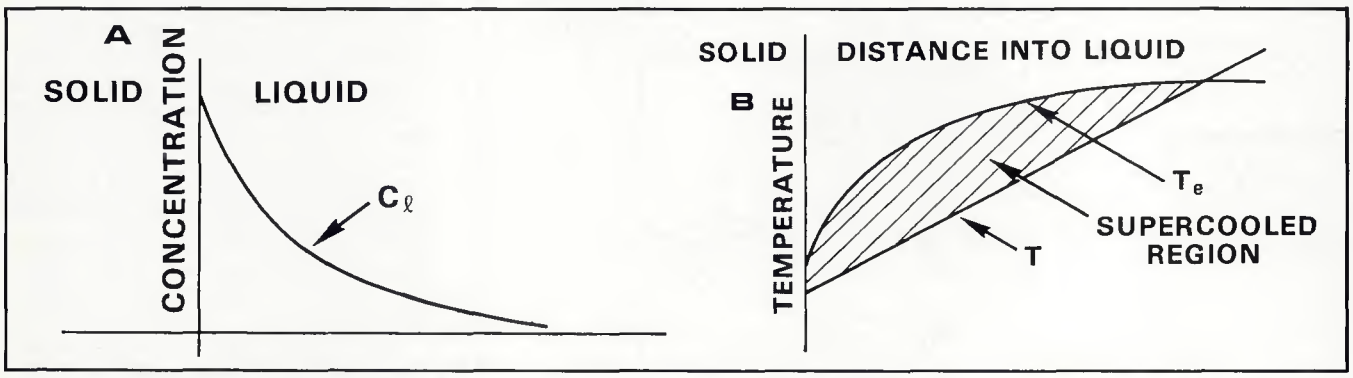

Fig. 3—Solute redistributions leading to constitutional supercooling. A—Distribution of solute in liquid; B—Constitutional supercooling

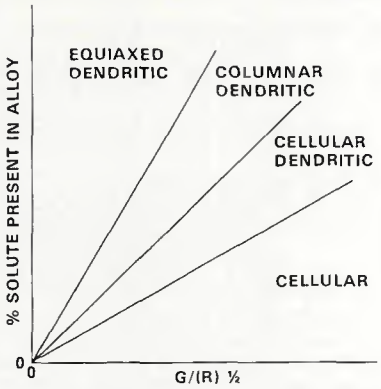

Fig. 4 – Effect of thermal gradient and solidification rate on solidification morphology

$$T = T_o - \frac{mC_o}{k_o} + G_1 x \qquad (4)$$

where T = actual temperature at a point x ahead of the interface
G_1 = thermal gradient in the liquid

The region within which the actual temperature is less than the effective liquidus temperature is said to experience constitutional supercooling, as shown in Fig. 3B. If the degree of supercooling is small, a cellular structure results. A greater degree of supercooling gives rise to a dendritic growth mode.

The extent of constitutional supercooling in a given alloy depends on the thermal gradient, G_1, and the solidification rate, R, in the liquid (Ref. 16). Tiller and Rutter (Ref. 19) have summarized the influence of these factors on the mode of solidification in the manner shown in Fig. 4. High thermal gradients and slow solidification rates favor cellular growth. Low values of $G_1/(R)^{1/2}$ indicate an increased tendency for constitutional supercooling and a dendritic mode of solidification. For a given solidification rate and material composition, the solidification morphology is influenced primarily by the thermal gradient in the weld pool. Thus, the theoretical basis for the production of an equiaxed weld structure is to reduce the thermal gradient to low enough values to allow heterogeneous nuclei to develop and grow.

Table 1—Welding Variables for Bead-on-Plate Welds

Identification	Welding Current (amperes)	Arc Voltage (volts)	Travel Speed (ipm)	Torch Gas (scfh)	Convective Cooling Gas (scfh)	Heat Input (kJ/in.)
Control	640	15	5	60 He	0	115
Convective cooling	640	15	5	60 He	200 He	115

Approach

It was noted during the literature survey that there were no studies on forced convection by jet impingement of weld metals deposited by high heat input welding processes. Therefore, the initial efforts focused on a heat transfer analysis to maximize convective cooling at the surface of large weld pools. Included in the analysis were the cooling gas (helium) and the number, size, shape and spacing dimensions of gas jet orifices. From the heat transfer analysis, a jet impingement plate was prepared by machining a 5 × 7 array of 0.060-in. (1.52-mm) diameter holes with a center-to-center hole spacing of 0.25 in. (6.35 mm) in a 1 × 2 × 0.03-in. (25.4 × 50.8 × 0.76-mm) copper sheet. The upstream edges of each gas orifice were slightly rounded to avoid vena contracta convergence downstream of the jet array. A special device was constructed to apply forced convective cooling during in-process welding – Fig. 5. The device consisted of a copper tube to supply gas to the jet plenum, an outer copper enclosure with provisions for water cooling, an inner jet plenum containing a baffle and screen to ensure even distribution of the gas and the jet impingement plate. The device was attached to the rear of a GTAW torch so that multiple gas jets would impinge perpendicular to the surface of the weld pool.

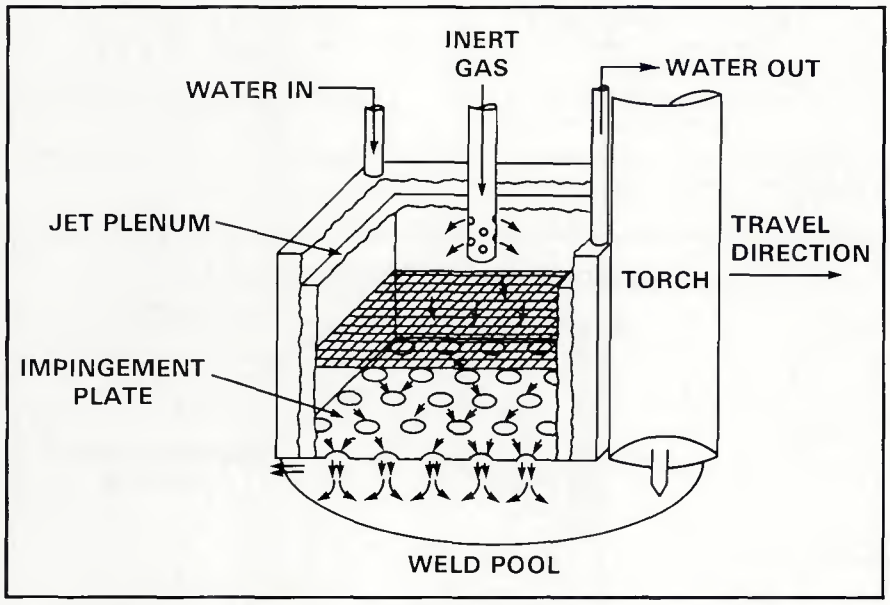

Fig. 5 – Device for forced convective cooling of weld pools

Experimental Procedures

The plate material used in this study was titanium alloy Ti-6Al-4V of 1-in. (25.4-mm) thickness. Prior to welding, the plate surfaces were degreased with acetone and rotary wire brushed. Using the welding variables in Table 1, autogenous bead-on-plate welds were produced by the automatic gas tungsten arc process at a heat input of 115 kJ/in. (4.5 kJ/mm). All welding variables were maintained constant; only the introduction of the convective cooling gas during welding was different.

Visual observations of the arc-shape and weld-pool geometry during welding were made via a weld-pool viewing system. The system consisted of a fiber optic device attached to the welding torch, appropriate filters, camera and video cassette recorder.

Temperature distributions in the weld pool were measured using tungsten, 5% rhenium/tungsten, 26% rhenium thermocouples. The thermocouple ends were dipped by hand into the center of the weld pool and held stationary until frozen into the advancing solidification front. Additional welds were produced in which the thermocouples were plunged in the weld pool to measure weld metal cooling rate. For all temperature measurements, the thermoelectromotive force was recorded on a fast response chart recorder.

Weld bead shape and HAZ width were characterized using light microscopy. Quantitative metallography was used

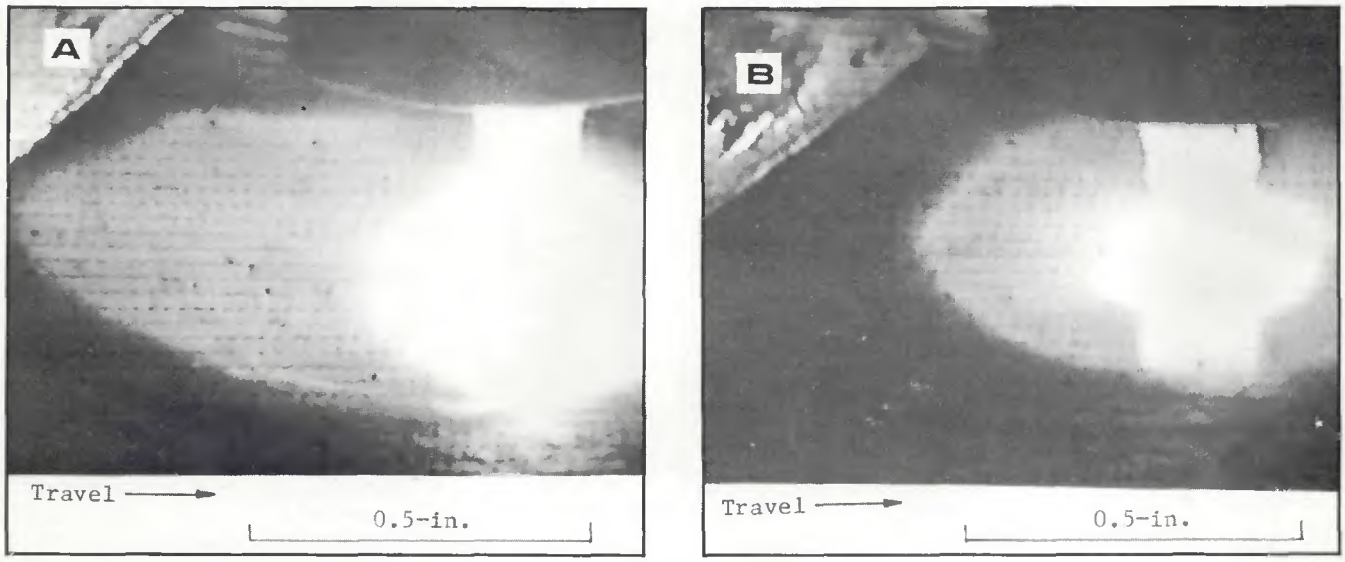

Fig. 6 — Gas tungsten arc shape and weld-pool geometry. A — Control; B — Convective cooling

to characterize the columnar grain size of the weld macrostructure and alpha platelet size of the weld microstructure.

Results

Arc Shape and Weld-Pool Geometry

The shape of the welding arc and weld-pool geometry during fabrication of the bead-on-plate welds is shown in Fig. 6. For welds produced without convective cooling, the welding arc was large and diffuse, assuming an approximately conical shape (Fig. 6A) typical of the GTAW process (Ref. 2). With the introduction of convective cooling, the welding arc was collimated and focused on a smaller area of the base plate. The shape of the arc was cylindrical near the tip of the tungsten electrode, changing to a smaller conical shape at the surface of the weld pool — Fig. 6B. Gas jet impingement on the trailing edge of the weld pool caused a change in weld pool geometry from tear-shaped (Fig. 6A) to elliptical (Fig. 6B), as seen on the weld-pool surface.

Temperature Distributions

A typical thermocouple trace is shown in Fig. 7. In welds where the thermocouple was dragged from a control weld pool into a convectively cooled weld pool, a decrease in peak surface temperature of approximately 140°F (60°C) was observed. In the liquid zone near the solid-liquid interface, forced convective cooling reduced the thermal gradient from 2200°F/in. (47°C/mm) to 1900°F/in. (41°C/mm). The effect of this reduction on constitutional supercooling is shown in Fig. 8. The effective liquidus temperature for Ti-6Al was calculated using Equation 3. The actual temperature ahead of the solid-liquid interface is also shown in Fig. 8 and was calculated using Equation 4 and the measured thermal gradients. By comparing the gradient of T_e with that of T, it can be seen that forced convective cooling increases the maximum length of the supercooled region from 0.005 in. (0.127 mm) to 0.007 in. (0.178 mm).

The thermal cycles in the solid zone are shown as a function of time in Fig. 9. For titanium, the temperature of interest is the start of the beta to alpha phase transformation, approximately 1600°F (871°C). At this temperature, forced convective cooling increases the solid-state cooling rate from 19°F/s (11°C/s) to 96°F/s (53°C/s). Figure 10 shows the continuous cooling transformation diagram developed previously for Ti-6Al-4V (Ref. 20). This diagram describes the beta to alpha decomposition kinetics. Superposition of the weld metal cooling rates measured in this study on the CCT diagram shows that the time for nucleation and growth of the alpha phase and the time to cool (to 1000°F (538°C)) are reduced with convective cooling. These results are presented in Table 2. Data for titanium welds fabricated at various heat inputs are also provided for comparison purposes (Ref. 21).

Bead Shape and Grain Size

Visual examination of the welds showed good weld bead contour with no indications of undercut from gas jet impingement. Forced convective cooling did modify the shape of the fusion zone (Fig. 11), increasing the depth of penetra-

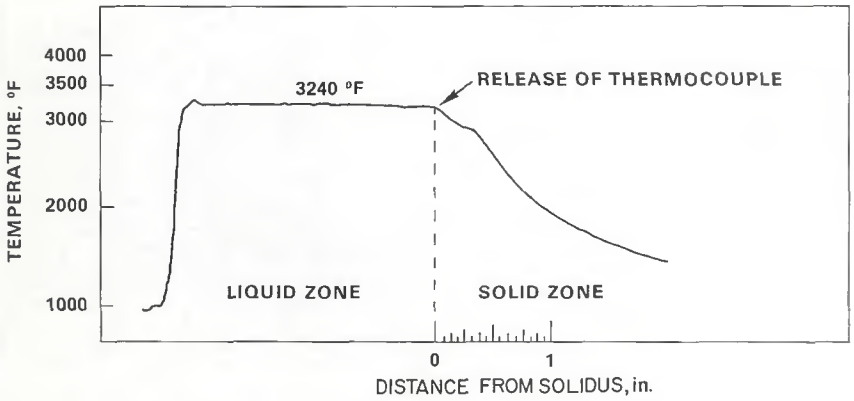

Fig. 7 — Temperature distribution for GTA weld pool

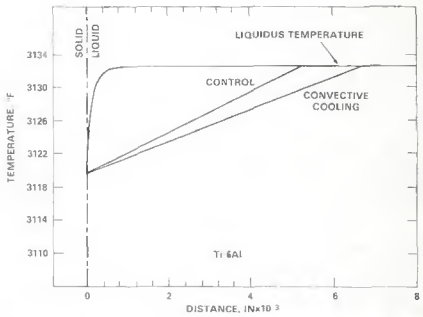

Fig. 8 — Effect of thermal gradients on constitutional supercooling

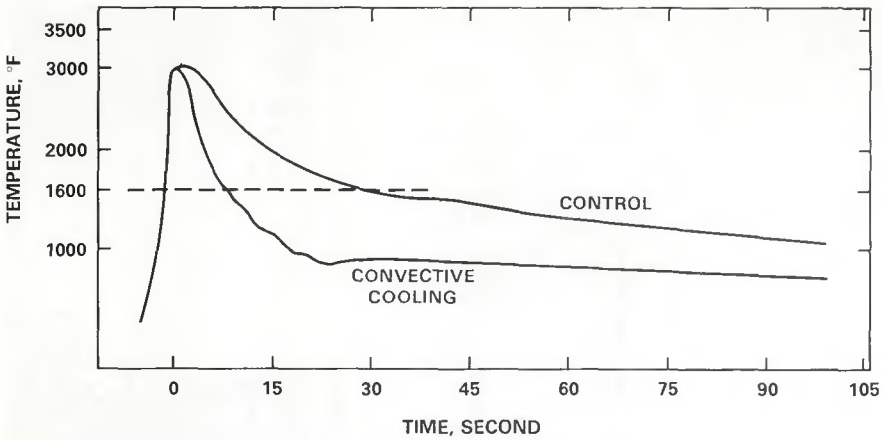

Fig. 9 — Weld metal cooling rate curves

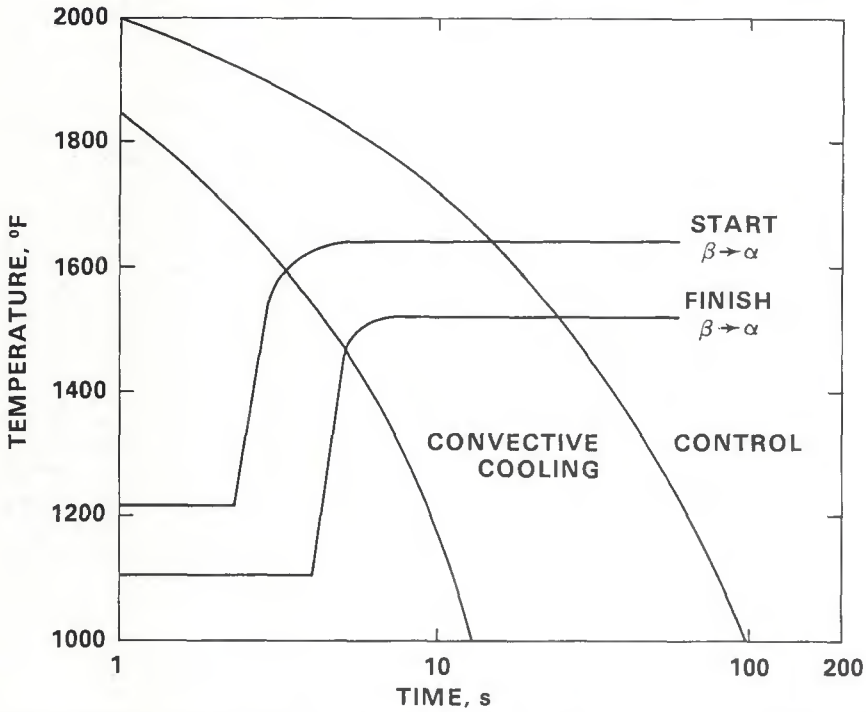

Fig. 10 — Cooling curves for GTA weld, superimposed on CCT diagram for Ti-6Al-4V (Refs. 20, 21)

tion and decreasing the width of the weld. The width of the weld HAZ was also reduced with convective cooling. This information is provided in Table 3.

Bead-on-plate welds produced without convective cooling exhibited a coarse columnar macrostructure, characteristic of high heat input welds (Ref. 2). Large single grains were observed to completely traverse the transverse fusion zone thickness — Fig. 11A. With the introduction of convective cooling, a predominantly equiaxed transverse macrostructure was obtained — Fig. 11B. This refinement extended through the depth of the fusion zone. Quantitative metallographic measurements of the weld macrostructure are provided in Table 4. The columnar grain size, as measured by the area, perimeter or diameter of columnar grains in the transverse (TS plane) cross-sections of Fig. 11, was reduced by a factor of 2 to 3 with convective cooling. Measurement of the columnar grains parallel to the welding direction (LT and LS planes) showed a slightly smaller reduction in columnar grain size with convective cooling. The macrostructure of the convectively cooled welds parallel to the welding direction (Fig. 12) exhibited a curved columnar structure, which is consistent with columnar grain development in an elliptically shaped weld pool (Refs. 5, 6).

Quantitative metallographic measurements of the alpha platelet size are provided in Table 5. Bead-on-plate welds produced with convective cooling to enhance cooling rate had a smaller alpha platelet size than the welds produced without convective cooling.

Discussion

From the literature review it was apparent that the temperature conditions in the weld pool exert a considerable influence on the resultant solidification structure. The method developed to apply forced convective cooling to large weld pools was expected to provide temperature conditions more favorable

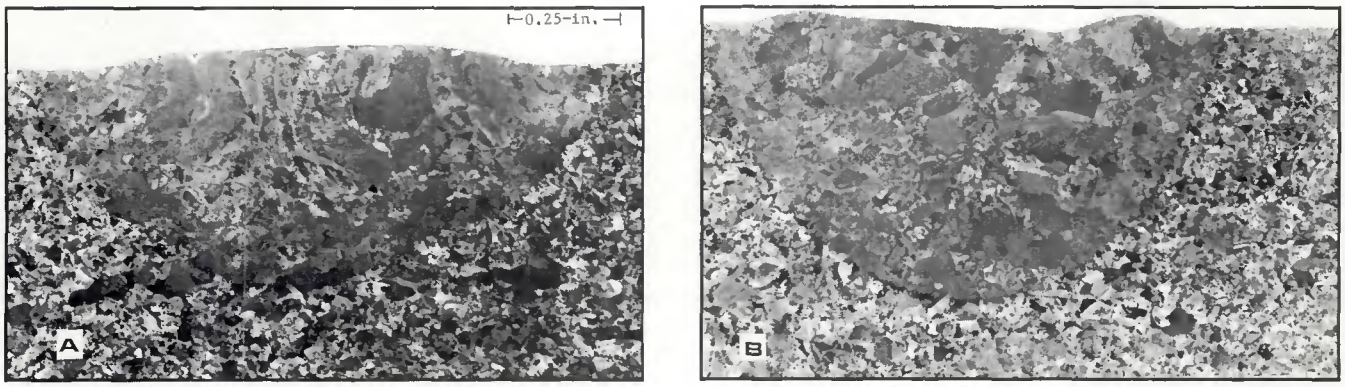

Fig. 11 — Photomacrographs showing weld macrostructure (TS plane). A — Control bead-on-plate weld; B — Convectively cooled bead-on-plate weld

for equiaxed growth by accelerating convective heat losses at the surface of the weld pool. The results of Fig. 8 show that the degree of supercooling ahead of the solid-liquid interface is increased as a result of the reduction in thermal gradients obtained with gas impingement. However, the maximum increase in the length of the supercooled region is so small (0.002 in./0.051 mm) that a columnar-to-equiaxed growth transition, as illustrated in Fig. 4, would not be expected.

Although forced convective cooling did not produce grain refinement by nucleation and growth, the method does form a refined weld metal macrostructure. Refinement is achieved by a change in weld pool geometry (Fig. 6) caused by gas impingement on the trailing edge of the weld pool. This change in pool shape ensures the survival of many more columnar grains (Fig. 11) and was effective in reducing the transverse columnar grain size by a factor of 2 to 3. In addition to a reduced grain size, forced convective cooling modified the shape of the bead—Fig. 11. Observations of the plasma arc during welding indicate that the change in bead shape is the result of arc constriction by jet impingement adjacent to the welding torch. The focused arc reduced the width of the weld pool (Fig. 6) and is believed to be responsible for the increase in the depth of penetration. Higher current densities and arc energy concentrations from plasma arc constriction (*i.e.* plasma arc welding) have been shown to produce higher depth-to-width ratios in a weld (Ref. 2), as was observed with convective cooling—Table 3.

The size of the alpha platelets in the weld microstructure is dependent on the continuous cooling transformation characteristics of the Ti-6Al-4V alloy and the weld metal cooling rate (Ref. 15). For bead-on-plate welds produced with jet impingement to enhance cooling rate,

Table 2—Transformation and Cooling Times from CCT Diagram

Identification	Heat Input (k)/in.)	Cooling Rate (1600°F) (°F/s)	Transformation Time (s)	Time to Cool (2000° to 1000°F) (s)
Control	115	19	11	100
Convective cooling	115	95	2	13
A[a]	156	5	25	185
B[a]	94	25	10	90
C[a]	62	39	4	30
D[a]	29	65	2	18

[a]See Ref. 21.

Table 3—Bead Shape and HAZ Width of GTAW Welds

Identification	Depth of Penetration (in.)	Weld Width (in.)	D/W Ratio	HAZ Width (in.)
Control	0.500	1.125	1:2.25	0.125
Convective cooling	0.625	0.970	1:1.6	0.062

Table 4—Columnar Grain Size of Weld Macrostructure

Identification	Plane	Area (in.^{2} × 10^{-3})	Perimeter (in. × 10^{-1})	Diameter (in. × 10^{-1})
Control	TS	9.3	4.4	1.7
Convective cooling	TS	2.8	2.2	0.8
Control	LT	4.6	3.1	1.0
Convective cooling	LT	2.2	2.1	0.7
Control	LS	2.8	2.6	0.9
Convective cooling	LS	1.3	1.6	0.5

Table 5—Alpha Platelet Size of Weld Microstructure[a]

Identification	Plane	Area (in.^{2} × 10^{-8})	Length (in. × 10^{-4})	Width (in. × 10^{-4})	ASTM Grain Size
Control	TS	0.9	2.0	0.6	14
Convective cooling	TS	0.4	1.6	0.4	15

[a]Measurements taken at depth of 1/16 in. below surface.

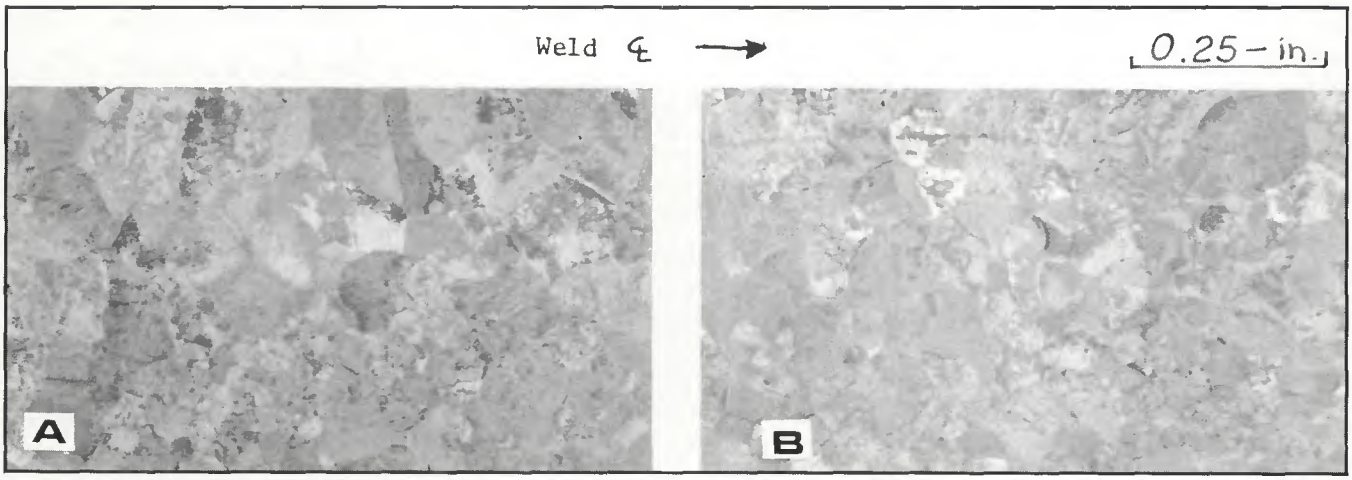

Fig. 12—Photomacrographs showing weld macrostructure (LT plane). A—Control bead-on-plate; B—Convectively cooled bead-on-plate weld. Note curved columnar grain development

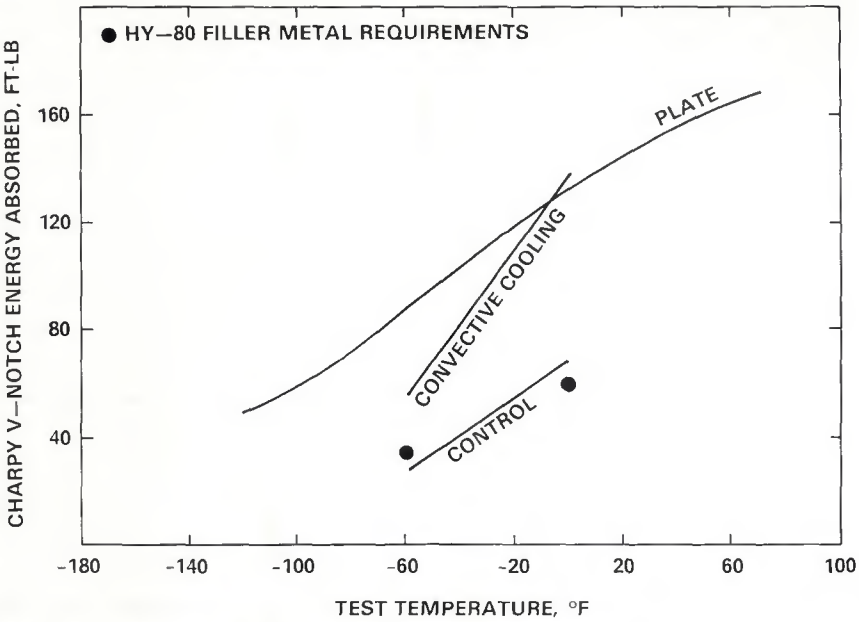

Fig. 13 — Charpy impact data for HSLA-80 GTAW autogenous welds (Ref. 22)

the time for nucleation and growth of the alpha phase is suppressed — Table 2. For this reason, the alpha platelets are narrower and shorter — Table 5. It should be noted that a smaller columnar grain size, as obtained with convective cooling, will also move the CCT curve to shorter times (Ref. 3). However, it was not possible to separate the effects of these two factors (smaller grain size and accelerated cooling) on transformation time.

Many alloys are cooling rate sensitive and the rate at which the weld metal cools can have a significant effect on weldment properties (Ref. 2). As shown in Table 2, the transformation cooling rate achieved with convective cooling at a heat input of 115 kJ/in. (4.5 kJ/mm) is comparable to heat input levels of 20–40 kJ/in. (0.8–1.6 kJ/mm) without convective cooling. In consideration of these factors, the results of this work were applied to accelerate cooling rates of thick section ASTM A710 HSLA steel weldments fabricated autogenously by the GTAW process at a heat input of 150 kJ/in. (5.9 kJ/mm). The Charpy V-notch results from this study (Ref. 22) are presented in Fig. 13. Typical plate properties, and HY-80 GTAW filler metal requirements (Ref. 23), are provided for comparison. These data show that the weldment produced with convective cooling had higher toughness values than the weldment produced without convective cooling, and easily meet HY-80 filler metal requirements.

Conclusions

In this work, a method has been developed to apply forced convection heat transfer by gas impingement to Ti-6Al-4V weld metals deposited by the GTAW process at a heat input of 115 kJ/in. (4.5 kJ/mm). The results of the application of this method indicate the following:

1. Forced convective cooling forms a refined weld metal macrostructure. Grain refinement is achieved by a change in weld-pool geometry caused by jet impingement on the trailing edge of the weld pool.

2. The weld metal cooling rate increases with forced convective cooling. By increasing the cooling rate, the time at transformation temperature is reduced and a finer weld metal microstructure is produced.

3. Forced convective cooling modifies the shape of the deposited weld bead. The depth-to-width ratio of the fusion zone increases and the width of the weld HAZ decreases.

4. With the introduction of forced convective cooling, the weld pool temperature decreases and thermal gradients in the fusion zone near the solid-liquid interface also decrease.

References

1. Kelsey, R. A., *et al.* 1984. Current welding research problems. Welding Research Council Bulletin 293, April 1984, p. 12.

2. *Welding Handbook.* Edited by C. Weisman, Seventh Edition, American Welding Society, Miami, Florida, 1976, Vols. 1 and 2.

3. Easterling, K. 1983. *Introduction to the Physical Metallurgy of Welding.* Butterworths, U.K., 1983.

4. MIL-STD-1689 (SH). December 1983. Fabrication, welding and inspection of ship structures, p. 75.

5. Davies, G. J., and Garland, J. G. 1975. Solidification structures and properties of fusion welds. *International Metallurgical Review 196,* pp. 83–106.

6. Garland, J. G. 1974. Weld pool solidification control. *Metal Construction* (4):121–127.

7. Simpson, R. P. 1977. Controlled weld pool solidification structure and resultant properties with yttrium inoculation of Ti-6Al-4V-2Sn welds. *Welding Journal* 56(3):67-s to 77-s.

8. Morgan-Warren, E. J. 1980. Weld metal solidification and its control by stirring. *Arc Physics and Weld Pool Behavior,* The Welding Institute, Cambridge, England, Vol. 1, pp. 325–334.

9. Kercher, D. M., and Tabakoff, W. 1970. Heat transfer by a square array of round air jets impinging perpendicular to a flat surface including the effect of spent air. *Journal of Engineering for Power* (1):73–82.

10. Metzger, D. E., and Korstad, R. J. 1972. Effect of crossflow on impingement heat transfer. *Journal of Engineering for Power* (1):35–42.

11. Sparrow, E. M., *et al.* 1975. Effect of nozzle-surface separation distance on impingement heat transfer for a jet in a crossflow. *Journal of Heat Transfer* (11):528–533.

12. Hollworth, B. R., and Berry, R. D. 1978. Heat transfer from arrays of impinging jets with large jet-to-jet spacing. *Journal of Heat Transfer* (5):352–357.

13. Birman, U. I., *et al.* 1983. Special features of welding aluminum alloys with artificial cooling of the joint by localized jets. *Welding Production* (8):23–25.

14. Beal, J. B., and Bodinger, M. A. October 1984. Electrostatic cooling applications. *Second Annual AIAA Aerospace Technology Symposium,* New Orleans, La., Vol. 7, Paper 84-044.

15. Baeslack, W. A., *et al.* 1984. Advances in titanium alloy welding metallurgy. *Journal of Metals* (5):46–58.

16. Savage, W. F., *et al.* 1965. Weld metal solidification mechanics. *Welding Journal* 44(4):175-s to 181-s.

17. Savage, W. F., and Aronson, A. R. 1966. Preferred orientation in the weld fusion zone. *Welding Journal* 45(2):85-s to 89-s.

18. Chalmers, B. 1964. *Principles of Solidification.* John Wiley and Sons, New York, N.Y.

19. Tiller, W. A., and Rutter, J. W. 1956. The effect of growth conditions upon the solidification of a binary alloy. *Canadian Journal of Physics,* Vol. 34, p. 96.

20. LeMoitre, F. 1970. Study of transformations in Ti-6Al-4V titanium alloy under continuous cooling. *Scientific Revue Metallurgy,* Vol. 67, pp. 563–574.

21. Lukens, W. E. DTNSRDC, unpublished data.

22. Lukens, W. E. April 1986. Mechanical properties of HSLA steel buried gas tungsten arc weldments. Paper presented at the 67th Annual AWS Convention, Atlanta, Ga.

23. MIL-E-23765/2C (SH). June 1983. Electrodes and rods, welding, bare, solid or alloyed core, low alloy steel, p. 7.